`

Optical properties of the substrate-buried spherical dipole nanoantenna

A. V. Dyshlyuk (orcid.org/0000-0001-5804-6579)[a,b]*, N.A. Inogamov (orcid.org/0000-0002-7703-4415)[c,d,e], O.B. Vitrik (orcid.org/0000-0002-5932-550X)[a]

[a] *Institute of Automation and Control Processes, Far Eastern Branch of the Russian Academy of Sciences (IACP FEB RAS), Vladivostok, 690041 Russia*

[b] *Vladivostok State University (VVSU), Vladivostok, 690041 Russia*

[c]*Landau Institute for Theoretical Physics of Russian Academy of Sciences, Moscow, 142432 Russia*

[d]*Joint Institute for High Temperatures of Russian Academy of Sciences, Moscow, 125412 Russia*

[e]*The Federal State Unitary Enterprise Dukhov Automatics Research Institute, Rosatom, Moscow, 127055 Russia*

**e-mail: anton_dys@iacp.dvo.ru*

Received
Revised
Accepted

Abstract — The paper studies the properties of a plasmonic nanoantenna in the form of a subwavelength metal sphere partly buried in a metal substrate with a hollow gap between the sphere and the substrate. Using a nickel sphere in a nickel substrate as an example, it is shown that imbedding a metal sphere deep into the substrate leads to the broadening and a strong red shift of its dipole resonance. Significant enhancement of the near electromagnetic field of the sphere in the gap region is demonstrated. The effect of all geometric parameters of the nanoantenna under study on its optical performance is studied. Enhanced transmission of a metal film with defects in the form of spherical particles embedded in it is demonstrated, which results from the leaking of the near electromagnetic field from the gaps to the opposite side of the film. The obtained results can find application in nanooptics for designing plasmonic nanoantennas for concentration, enhancement and redistribution of the electromagnetic field.

Keywords: Mie scattering, scatterer on substrate, dipole resonance, spherical nanoantenna, plasmonics, nanooptics.

`

INTRODUCTION

A plasmonic particle of subwavelength dimensions located on a suitable substrate is a basic building block for a vast number of functional photonic structures and elements [1-3] including metamaterials and metasurfaces [4-6], bio- and chemosensors [7-10], surface enhanced Raman scattering platforms [10-14], to name just a few. For this reason, the problem of the interaction of light with a particle on a substrate has been long in the focus of attention of many scientists and research groups [15-32].

From the standpoint of mathematical physics, such a problem is not simple, since the presence of a substrate violates the symmetry of the geometry under consideration even for regular-shaped particles, and also due to the fact that the solution to the problem depends significantly on the particular shape of the particle, its orientation with respect to the substrate, and on the optical properties of the substrate. The simplest approach to this problem, applicable to particles much smaller than the wavelength, is to model the particle as a point dipole.

Beginning with the pioneering treatment of the problem of a vertically oriented dipole above a flat and lossy surface by Sommerfeld [16], many researchers have addressed the problem of dipole radiation in a half space [17-19]. However, this approach is applicable only in the case where the electromagnetic field can be considered uniformly distributed over the particle volume and retardation effects do not come into play, and also if the particle is not located too close to the substrate. As the particle nears the substrate the diploe approximation begins to fail because the contributions of higher-order multipoles due to the interaction of the particle with the substrate become significant [15].

The problem of light scattering by small particles, with due account of their finite sizes, has been treated by many researchers, who primarily considered particles of regular geometries including cylinders, spheres and spheroids. For example, in [20] the authors solved the problem of light scattering by a sphere above a perfectly reflecting mirror was solved, while in [21, 22] Fresnel formulas were used to handle cases of non-perfectly reflecting substrates. In some works, the problem of light scattering by a spherical particle over a substrate is reduced to two problems: light scattering by a sphere in a homogeneous medium (Mie theory) and reflection of spherical waves from the substrate [23, 24].

A large number of works on light scattering by particles on substrates use exact integral equations for the electromagnetic field, which are solved by standard numerical methods. The integral equations are derived from the Maxwell's differential equations in combination with specified boundary conditions, with a frequent use of the extinction theorem from physical optics [25]. Although this theorem was initially used mainly to solve the problem of light scattering by irregular rough surfaces, many authors adapted this technique to calculate near and far electromagnetic fields when light is scattered by small metal particles on conducting substrates, taking into account multiple interactions of particles with the substrate [26, 27]. This approach enabled the study of the effect of particle sizes, their distance to the substrate, and the optical properties of the substrate on the peculiarities of light scattering [28, 29], including the possibility of exciting surface plasmon-polariton waves on the conducting substrates [30-32].

It should be noted, however, that in most studies where the problem of light scattering by a particle on substrate is treated, the particle is assumed to be located either directly on the substrate or at some small distance above it. The case when a spherical plasmonic particle is partially or completely

`

buried in the substrate with some hollow gap between the particle and the substrate material has not been given sufficient attention, despite the fact that it is not an unlikely arrangement in plasmonic and nanophotonic functional structures. The aim of this work is to study the optical properties of a substrate-buried dipole plasmonic nanoantenna in the form of a subwavelength metallic spherical particle, deeply embedded in a metallic substrate, as well as the dependence of these properties on the geometric parameters of the nanoantenna.

METHODOLOGY OF THE STUDY

The 3D geometry of the plasmonic nanoantenna under study is shown schematically in Fig.1 (side view in the plane of the **E** vector of the incident wave). A spherical metal particle (radius R) is embedded in a metal substrate with a small hollow gap and irradiated by a normally incident plane wave of unit amplitude. For the material of the particle and substrate we chose nickel, since this metal has pronounced ferromagnetic properties, the combination of which with the optical response of the plasmonic nanoantenna opens up intriguing possibilities of creating opto-magnetic multifunctional devices, such as biosensors that can be remotely controlled by external magnetic fields [33]. The data on the complex permittivity of nickel are taken from the reference [34].

In this paper, the problem of scattering of an incident electromagnetic wave by a substrate-buried nickel nanoantenna is solved numerically using the finite difference time domain (FDTD) method. To resolve adequately the rounded surface of the nanoantenna, we locally refine the computational grid with an appropriate step in the range of 0.5 - 1 nm. Due to the orientation of the incident wave and the symmetry of the geometry under study, only its quarter needs to be modeled with a symmetric boundary condition across the z-axis and an antisymmetric one across the y-axis (on one side). On the other side in the transverse directions as well as in the longitudinal direction, the computational domain is bounded by absorbing boundary conditions in the form of perfectly matched layers (PML).

RESULTS AND DISCUSSION

To gain insight into the performance of the substrate buried spherical nanoantenna let us follow the evolution of its spectral response as the metal sphere nears and then gets imbedded into the substrate. In Fig.2 we plot the spectral dependences of the maximum near-field amplitude (at the point near the sphere where it is the strongest) starting from a solitary sphere in vacuum (curve 1), and then for the sphere near (curve 2) and vey near (curve 3) the substrate (shown in the insets are the corresponding distributions of the electric field amplitude in the plane of the electric field vector of the incident wave at the resonant wavelength where the near field around the sphere is the strongest).

It can be seen from the figure, that for a solitary sphere in vacuum, a weak dipole resonance, strongly damped by a large imaginary part of the dielectric permittivity of nickel is observed at $\lambda \sim 470$ nm (inset 1). However, as the sphere approaches the substrate, the resonance becomes more pronounced and the near field of the sphere is noticeably enhanced (curves 2, 3). This effect is explained by the effect of the conducting substrate: the field from the charges induced on its surface can be described by the field of an image dipole located in the substrate, which tends to enhance the dipole moment induced by the incident wave in the spherical particle. If the sphere is not too close to the substrate (curve 2), its near field is enhanced without significant changes to its distribution which

`

remains to be characteristic of the dipole resonance (inset 2). However, as the gap between the sphere and the substrate approaches zero, the near field pattern is significantly altered both by the field of the image dipole and by increasingly contributions from the higher order multipole moments with the field maximum shifting to the gap region (inset 3). For a 3 nm gap between the surface of the sphere and the substrate, an approximately twofold enhancement of the near field is observed compared to the case of a solitary sphere in vacuum (compare insets 1 and 3).

As the sphere begins to penetrate into the substrate, an even greater enhancement of the near field is observed in the gap region and the resonance becomes even more pronounced (curves and insets 4-7). The resonant wavelength remains unchanged at first (curve and inset 4) but with further deepening of the sphere into the substrate the resonance is strongly red shifted and broadened (curves 5, 6, and 7). When the sphere is 75% buried in the substrate (curve 7), the resonance maximum shifts to a wavelength of $\lambda \sim 1000$ nm so that the near-field amplitude increases monotonically over the entire 400-1000 nm wavelength range of interest. The highest, more than 3-fold near-field enhancement in the gap is observed at a wavelength of $\lambda = 700$ nm for the sphere 25% embedded in the substrate (curve 5).

To illustrate the effect of the size of the sphere on the spectral response of the substrate-buried nickel nanoantenna, we plot in Fig. 3 the spectral dependences of the maximum near-field strength in a 5 nm wide gap for a sphere ~25% in the substrate with R ranging from 30 nm to 70 nm.

As can be seen, with increasing radius of the spherical particle, a monotonic red shift of the resonance is observed, with a gradual increase in the maximum value of the near-field strength up to its ~ 4-fold enhancement (as compared to a solitary nickel sphere in vacuum) at R = 70 nm. As can be guessed from the character of the curve for R = 70 nm, with a further increase in the size of the sphere, the growth of the near-field amplitude saturates and slows down, while the resonance shifts further into the infrared range and broadens even more.

To illustrate the effect of the varying gap between the sphere of a constant radius and the material of the substrate, Fig. 4 shows the calculated spectral dependences of the maximum near-field amplitude in the gap ranging from 3 to 10 nm in width for the R=50 nm sphere 50% buried in the substrate.

As can be seen from the figure, decreasing the gap width at a constant R has approximately the same effect as decreasing the sphere radius at a constant gap (Fig. 3): the resonance broadens and strongly red shifts, which is accompanied by an increase in the near-field amplitude.

We note that in practice, when fabricating a substrate-buried spherical nanoantenna, the spherical particle will not "levitate" in a substrate cavity, but must be in some way attached to the substrate. This naturally raises the question of the effect of the attaching stem on the optical characteristics of the nanoantenna. To answer this question, Fig. 5 shows the results of calculating the spectral dependences of the highest near-field amplitude in a 5 nm wide gap for different sizes of the attaching stem, which is chosen to be in the form of a cylinder spanning the gap with its axis passing through the center of the sphere perpendicular to the substrate surface (see the inset to Fig. 5).

It is evident from the figure that up to the large stem radii (r=40-50 nm), approaching that of the spherical particle itself, the base has a very weak effect on the spectral response of the nanoantenna. This is explained by the distribution of the near field in the gap: the field maxima fall on the upper and lower sides of the gap, while in the region of the gap where it is spanned by the attaching stem,

`

the field is very weak even in the absence of the stem. Therefore, covering the gap with the stem does not affect the optical properties of the nanoantenna as far as the stem is not so large that it also covers the lateral regions of the gap.

The enhanced near field in the gap can be transformed into propagating electromagnetic waves if such waves can exist in the region immediately behind the spherical particle. To illustrate this fact, and also as a possible application of the proposed substrate-buried nanoantenna, Fig. 6 shows the results of a numerical study of the optical properties of a nickel film on a glass substrate with a large number of randomly located defects in the form of spherical nickel particles embedded in the film (Fig. 6a). To simplify the calculations, the array of the randomly located defects is approximated by an infinite ordered array of rectangular symmetry with a cubic unit cell bounded in the transverse directions by periodic boundary conditions with a period of Δ=130 nm. Such a period is subwavelength and small enough to exclude any collective effects due to the orderliness of the simulated array. In the longitudinal direction, the cell, as in the above situation of a single nanoantenna in a bulk substrate, is bounded by absorbing boundary conditions in the form of perfectly matched layers (PML).

As can be seen from Fig. 6b and 6d, the enhanced near field in the gaps of each defect leaks to the other side of the film and propagates further as travelling radiation. Waves from individual defects interfere constructively (in the propagation direction of the incident wave), giving a single transmitted wave of sizable amplitude. This gives rise to the 5 to 10-fold enhancement of transmittance of the nickel film with defects (Fig. 6c), as compared to that of a smooth nickel film of the same thickness without defects. Since the enhanced transmission is a result of the enhanced near field in the gap leaking to the other side of the film, the transmission spectrum essentially mimics the spectral behavior of the near-field amplitude in the gap. The defects in the film also affect the reflected wave, halving the reflection coefficient of the defected film as compared to that of the smooth film, the latter being ~70% at λ~700 nm.

CONCLUSIONS

Thus, in this work we studied the optical properties of the substrate-buried plasmonic dipole nanoantenna in the form of a subwavelength spherical metal particle embedded in a metal substrate with a hollow gap between the particle and the substrate material. Using a nickel sphere in a nickel substrate as an example, we showed that imbedding the spherical nanoantenna into the substrate leads to broadening and a strong red shift of its dipole resonance, which is accompanied by a redistribution of the near field of the nanoantenna into the gap region, where it experiences a 3 to 4-fold enhancement compared to the case of a solitary sphere in vacuum. The effect of the sphere radius ranging from 30 to 70 nm, the gap width ranging from 3 to 10 nm, and the size of the stem (by which the sphere is attached to the substrate) on the optical properties of the substrate-buried nanoantenna is examined. The conversion of the near electromagnetic field in the gap into propagating electromagnetic radiation is demonstrated using the example of a nickel film with defects in the form of spherical nickel particles embedded in it. It is shown that the presence of defects brings about up to 10-fold increase in the film transmittance as compared to the film without defects. The results obtained in the work can find application in plasmonics, nanooptics and nanophotonics for designing nanoantennas serving to concentrate, enhance or redistribute electromagnetic field.

`

FUNDING

The presented study is performed within the state task of IACP FEB RAS (121021600267-6, FWFW-2021-0001).

CONFLICT OF INTEREST

The authors declare that they have no conflicts of interest.

`

REFERENCES

1. Tonkaev, P., & Kivshar, Y., *JETP Letters*, 2020, vol. 112, no. 10, p. 615.
2. Berestennikov, A., Pushkarev, A. P., & Makarov, S. V., *Bulletin of the Russian Academy of Sciences: Physics*, vol. 86, Suppl. no. 1, p. 20.
3. Melnik, N. N., Sherstnev, I. A., & Tregulov, V. V. *Bulletin of the Russian Academy of Sciences: Physics*, 2021, vol. 85, p. 990.
4. Zhang, G., Lan, C., Bian, H., Gao, R., & Zhou, J., *Optics Express*, 2017, vol. *25*, no. 18, p. 22038.
5. Holloway, C. L., Kuester, E. F., Gordon, J. A., O'Hara, J., Booth, J., & Smith, D. R., *IEEE antennas and propagation magazine*, 2012, vol. *54*, no. 2, p. 10.
6. Alvarez-Fernandez, A., Cummins, C., Saba, M., Steiner, U., Fleury, G., Ponsinet, V., & Guldin, S., *Advanced Optical Materials*, 2021, vol. *9*, no. 16, p. 2100175.
7. Aristov, A. I., Zywietz, U., Evlyukhin, A. B., Reinhardt, C., Chichkov, B. N., & Kabashin, A. V., *Applied Physics Letters*, 2014, vol. 104, no. 7.
8. Kuznetsov, A. I., Evlyukhin, A. B., Gonçalves, M. R., Reinhardt, C., Koroleva, A., Arnedillo, M. L., ... & Chichkov, B. N., *ACS nano*, 2011, vol. 5, no. 6, p. 4843.
9. Su, X., Gao, L., Zhou, F., & Duan, G., *Sensors and Actuators B: Chemical*, 2017, vol. *251*, p. 74.
10. Yockell-Lelièvre, H., Lussier, F., & Masson, J. F., *The Journal of Physical Chemistry C*, 2015, vol. *119, no.* 51, p. 28577.
11. Wu, J., Yang, X., & Fang, J., *Particle & Particle Systems Characterization*, 2019, vol. *36, no.* 8, p. 1900268.
12. Christie, D., Lombardi, J., & Kretzschmar, I., *The Journal of Physical Chemistry C*, 2014, vol. *118, no.* 17, p. 9114.
13. Zhang, H., Zhou, F., Liu, M., Liu, D., Men, D., Cai, W., ... & Li, Y., *Advanced Materials Interfaces*, 2015, vol. *2, no.* 9, p. 1500031.
14. Kukushkin, V. I., Astrakhantseva, A. S., & Morozova, E. N. *Bulletin of the Russian Academy of Sciences: Physics*, 2021, vol. 85, p. 133.
15. Moreno, F., Saiz, J. M., & González, F., Light Scattering by Particles on Substrates. Theory and Experiments, chapter in *Light scattering and nanoscale surface roughness*, 2007, p. 305-340.
16. A. Sommerfeld, Partial differential equations in physics, New York, Academic Press, 1967.
17. Chew, W.C. Waves and fields in inhomogeneous media., Van Nostrand Reinhold, 1990.
18. Felsen, L. B., & Marcuvitz, N. Radiation and scattering of waves, vol. 31, John Wiley & Sons, 1994.
19. Novotny, L.: Principles of nano optics, Cambridge University Press., 2006.
20. Nahm, K. B., & Wolfe, W. L., *Applied optics*, 1987, vol. 26, no. 15, p. 2995.
21. Weber, D. C., & Hirleman, E. D. *Applied optics*, 1988, vol. *27, no.* 19, p. 4019.
22. Moreno, F., Saiz, J. M., Valle, P. J., & González, F., *Applied physics letters*, 1996, vol. *68*, no. 22, p. 3087.
23. Bobbert, P. A., & Vlieger, J., *Physica A: Statistical Mechanics and its Applications*, 1986, vol. 137, no. 1-2, p. 209.
24. Bobbert, P. A., Vlieger, J., & Greef, R. *Physica A: Statistical Mechanics and its Applications*, 1986, vol. *137, no.* 1-2, p. 243.
25. Vesperinas, M. N. Scattering and diffraction in physical optics., World Scientific Publishing Company, 2006.
26. Valle, P. J., González, F., & Moreno, F., *Applied optics*, 1994, vol. 33, no. 3, p. 512.
27. Valle, P. J., Moreno, F., Saiz, J. M., & González, F., *Physical Review B*, 1995, vol. *51, no.* 19, p. 13681.

`

28. Saiz, J. M., Valle, P. J., González, F., Ortiz, E. M., & Moreno, F., *Optics letters*, 1996, vol. 21, no. 17, p. 1330.
29. Valle, P. J., Moreno, F., Saiz, J. M., & Gonzalez, F. *IEEE Transactions on Antennas and Propagation*, 1996, vol. *44, no.* 3, p. 321.
30. Valle, P. J., Moreno, F., & Saiz, J. M., *JOSA A*, 1998, vol. *15, no.* 1, p. 158.
31. Dyshlyuk, A. V., Proskurin, A., Bogdanov, A. A., & Vitrik, O. B., *Nanomaterials*, 2021, vol. 11, no. 11, p. 2937.
32. Dyshlyuk, A. V., Bogdanov, A. A., & Vitirk, O. B., *Computer Optics*, 2020, vol. *44, no.* 6, p. 893.
33. Chen, J., Albella, P., Pirzadeh, Z., Alonso-González, P., Huth, F., Bonetti, S., ... & Hillenbrand, R., *Small*, 2011, vol. *7, no.* 16, p. 2341.
34. Haynes, William M. *CRC handbook of chemistry and physics*. CRC press, 2016.

`

FIGURE CAPTIONS

Fig. 1 Schematic drawing of the arrangement under study and its parameters (1 – vacuum, 2 – nickel)

Fig. 2 Spectral dependences of the maximum electric field amplitude (in a point near the sphere where it is the strongest) for various locations of the R=50nm nickel sphere with respect to the nickel substrate: (1) – isolated sphere in a vacuum without the substrate, (2) – sphere with a separation of 10 nm between its surface and the substrate, (3) – same as (2), but the separation is 3 nm. Curves (4) – (7) are for the sphere imbedded in the substrate with a 5 nm gap: (4) – h=50nm, (5) – h=25nm, (6) – h=0nm, (7) – h=-25nm. Shown in the correspondingly numbered insets are the distributions of the electric field amplitude at the resonant wavelengths (when the near field around the sphere is the strongest).

Fig. 3 Spectral dependences of the maximum electric field amplitude for various radii of the sphere ~25% buried in the substrate with a gap of 5 nm.

Fig.4 Spectral dependences of the maximum electric field amplitude for the sphere ~50% buried in the substrate with various gap width ranging from 3 to 10 nm, R=50 nm.

Fig. 5 Spectral dependences of the maximum electric field amplitude for the sphere with R=50 nm, ~50% buried in the substrate with a gap of 5 nm and attached to the substrate with a cylindrical nickel stem of various radii.

Fig. 6 Numerical simulation results for a nickel film on a glass substrate with defects in the form of nickel spheres partly buried in the film: (a) – simulated geometry in side view (1 – vacuum, 2 – nickel, 3 – glass substrate, R=50 nm, gap=5 nm, r=20 nm, h=54 nm, th=60 nm, Δ=130 nm); (b) – distribution of the electric field amplitude in the plane of the **E** vector at λ=1000 nm; (c) – calculated transmission spectrum of the nickel film with defects; (d) – distribution of the electric field amplitude at λ=1000 nm with a changed color scale to make the leaking of the electromagnetic field from the gaps into the glass clearly visible.

`

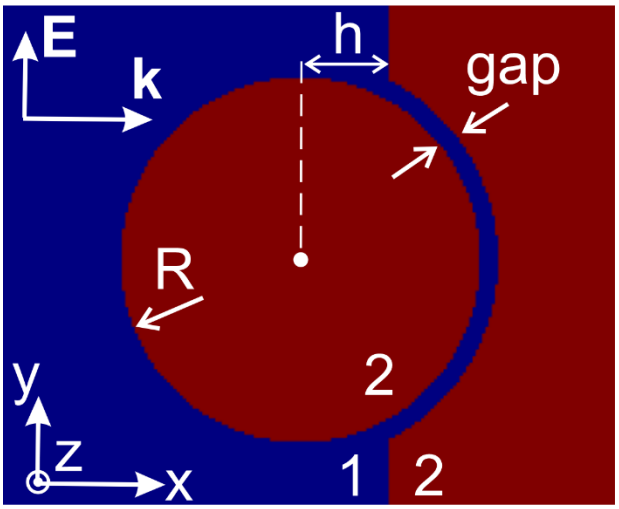
E
k
h
gap
R
2
y
z
x
1
2

Fig. 1

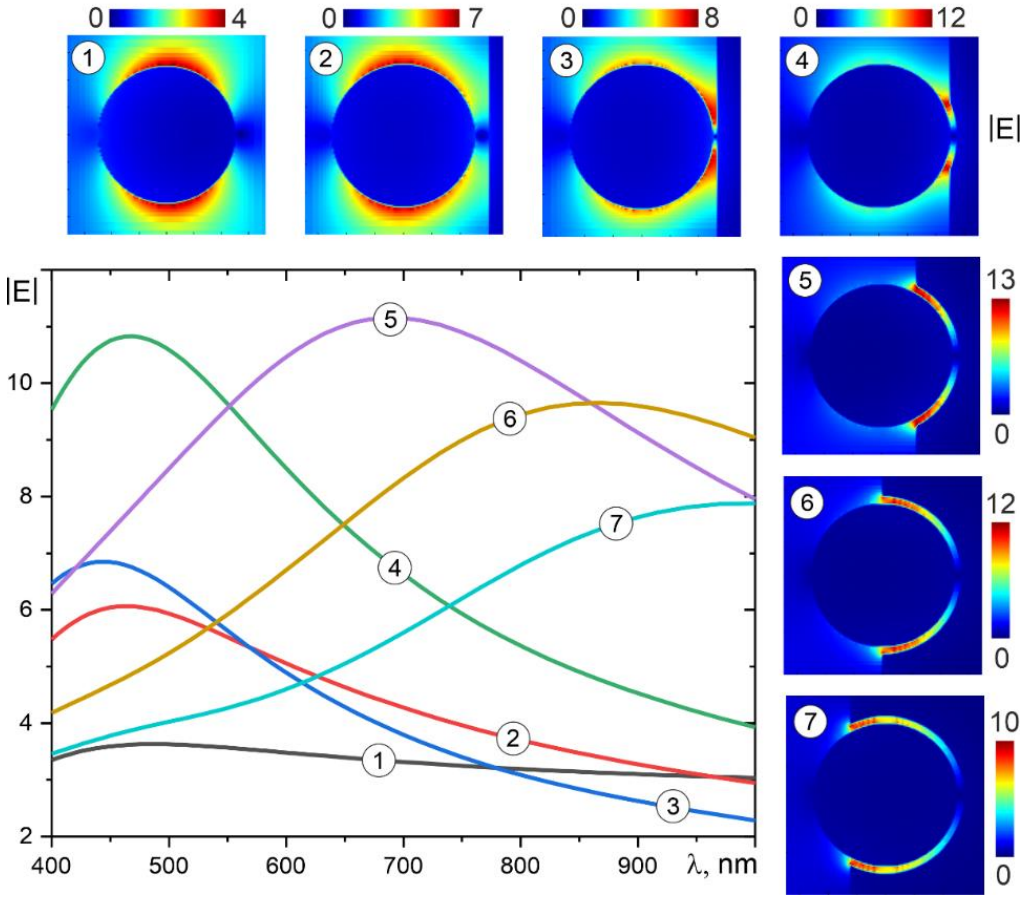
0
4
1
0
7
2
0
8
3
0
12
4
|E|
|E|
10
8
6
4
2
400
500
600
700
800
900
λ, nm
5
6
7
4
2
1
3
5
13
0
6
12
0
7
10
0

Fig. 2

`

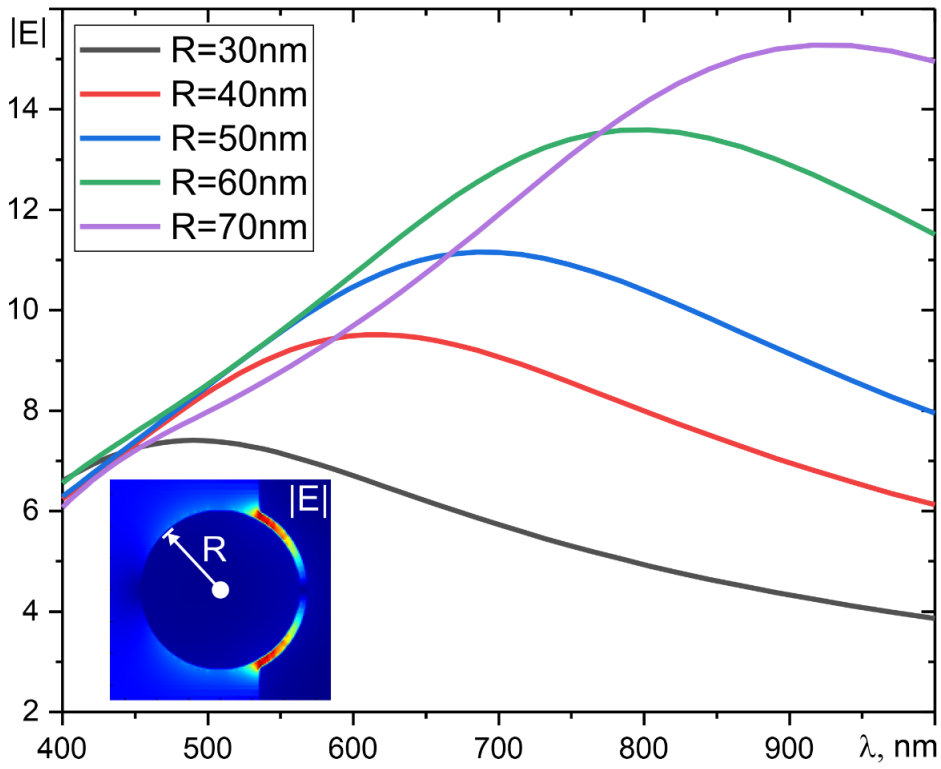
|E|
R=30nm
R=40nm
R=50nm
R=60nm
R=70nm
14
12
10
8
6
4
2
400
500
600
700
800
900
λ, nm
|E|
R

Fig.3

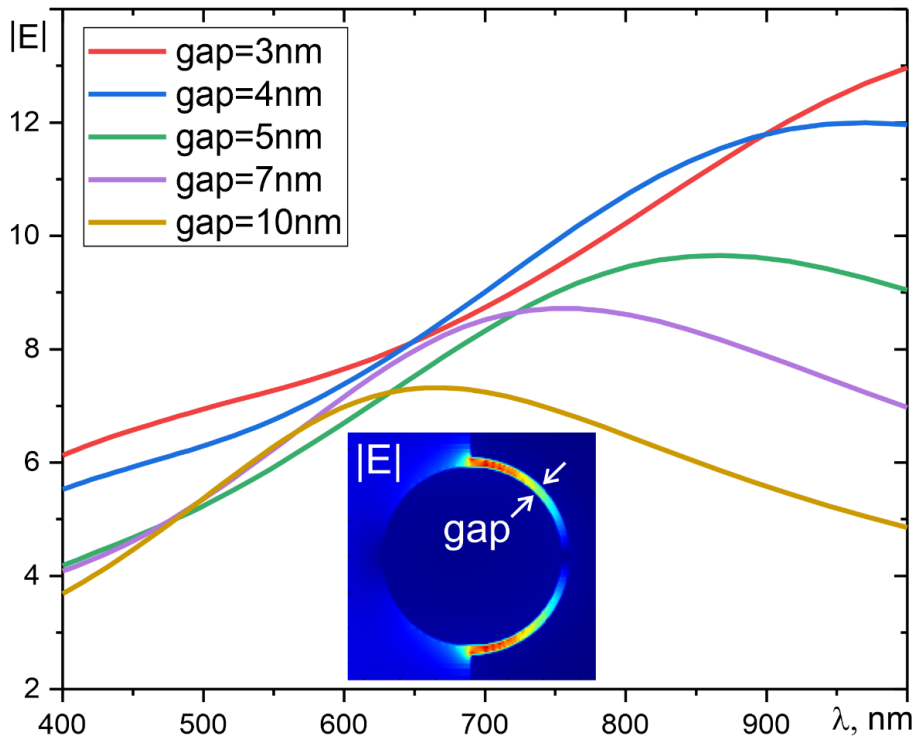
|E|
gap=3nm
gap=4nm
gap=5nm
gap=7nm
gap=10nm
12
10
8
6
4
2
400
500
600
700
800
900
λ, nm
|E|
gap

Fig. 4

`

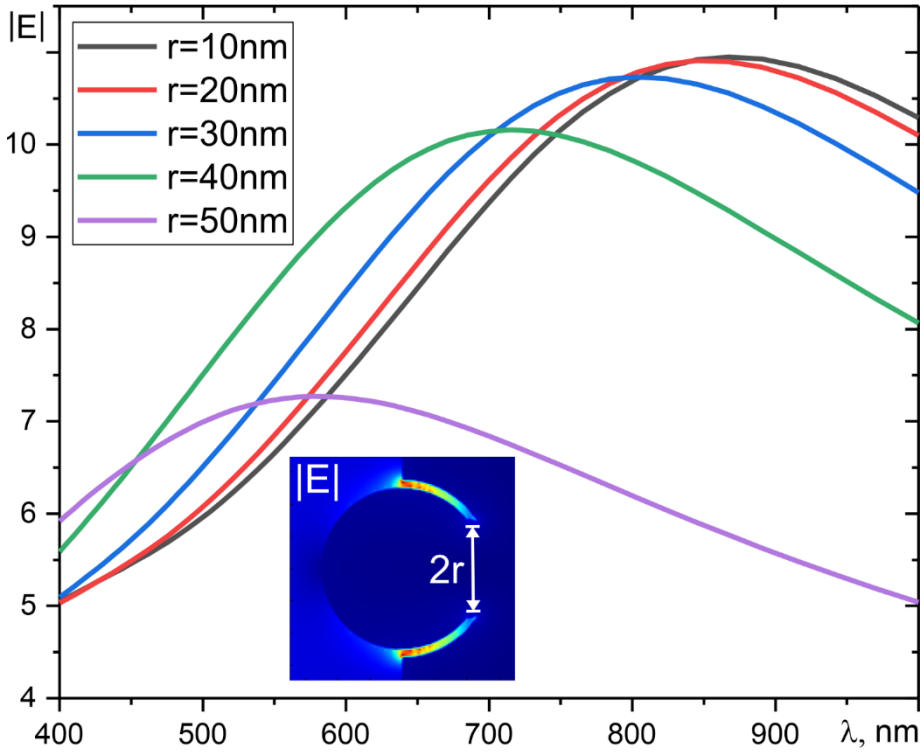
|E|
r=10nm
r=20nm
r=30nm
r=40nm
r=50nm
|E|
2r
λ, nm

Fig. 5

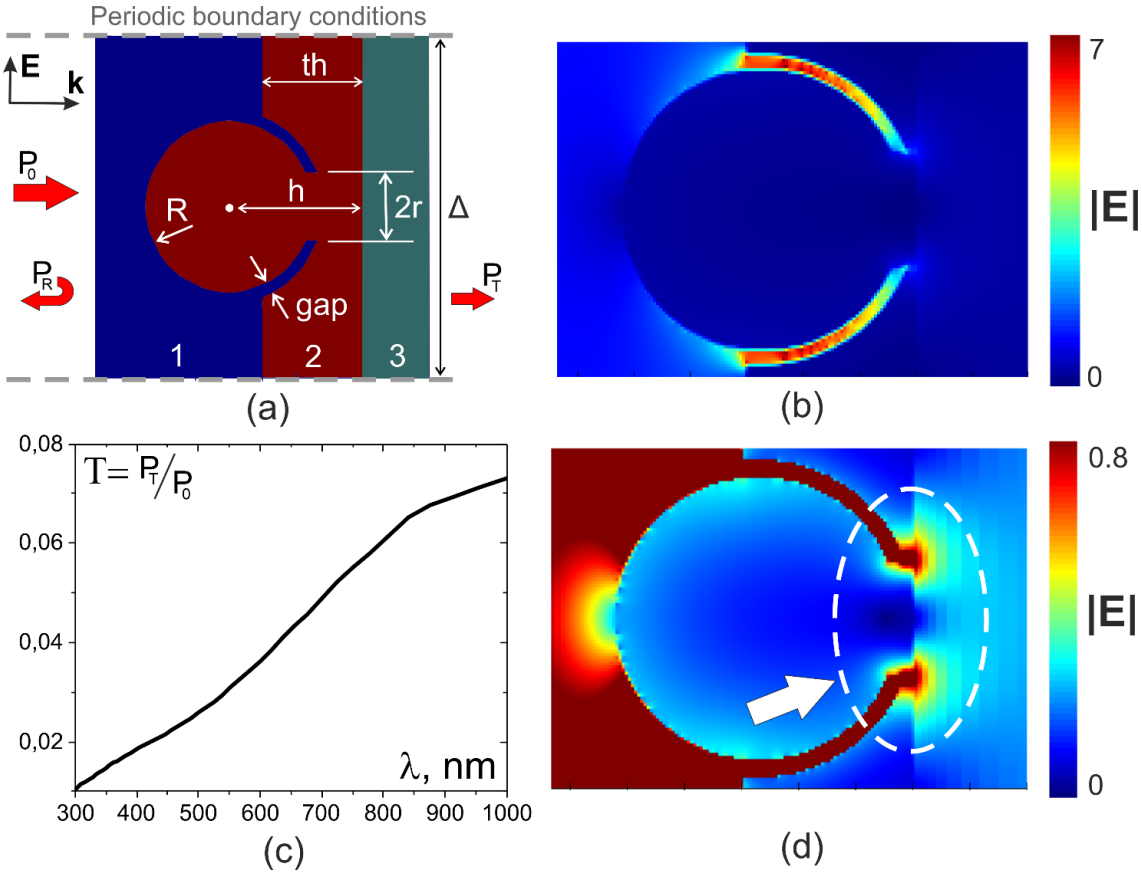
Periodic boundary conditions
E
k
P0
R
h
th
2r
Δ
PR
PT
gap
1
2
3
(a)
7
|E|
0
(b)
T= PT/P0
λ, nm
(c)
0.8
|E|
0
(d)

Fig.6